Reviews in Mineralogy & Geochemistry
Vol. 62, pp. 397-420, 2006

The Effect of Water on Mantle Phase Transitions

Eiji Ohtani and K. D. Litasov

Institute of Mineralogy, Petrology and Economic Geology
Tohoku University
Sendai, Miyagi-ken 980-8578, Japan
e-mail: ohtani@mail.tains.tohoku.ac.jp

INTRODUCTION

Water has played an important role in the Earth's evolution. The incorporation of water as hydroxyl into solid mineral phases or as coexisting hydrous fluids and melts affects the chemical and physical properties of crust and mantle constituents, i.e., it weakens rocks and minerals, reduces viscosity and strength of the materials, and depresses dramatically the melting temperature of silicate minerals (e.g., Karato 1990; Inoue 1994; Hirth and Kohlstedt 1996; Chen et al. 1998; Kubo et al. 1998; Mei and Kohlstedt 2000). Many recent studies have suggested the possible existence of water in the Earth's mantle especially in the transition zone (e.g., Smyth and Frost 2002; Ohtani et al. 2004; Litasov et al. 2005a; Hae et al. 2006), where wadsleyite and ringwoodite can accommodate up to 3 wt% of H_2O in their structures (e.g., Kohlstedt et al. 1996). Low-velocity zones observed seismologically at the top of the 410 km discontinuity may indicate the existence of trapped high-density melt (e.g., Revenaugh and Sipkin 1994; Song et al. 2004; Matsukage et al. 2005; Sakamaki et al. 2006), which is likely to be hydrous as it is not possible to melt the base of the upper mantle without water at these conditions. Electrical conductivity anomalies in the upper mantle and transition zone that are related to subduction zones have also been interpreted as an effect of water in the mantle (e.g., Fukao et al. 2004; Tarits at el. 2004; Hae et al. 2006; Koyama et al. 2006). Studies of the kinetics of the hydrous olivine-wadsleyite transformation (Ohtani et al. 2004; Hosoya et al. 2005) seem to be consistent with seismological observations (e.g., Koper et al. 1998) that indicate the absence of a metastable olivine wedge in subducting slabs. Such a metastable wedge would be expected as a result of the sluggish olivine-wadsleyite transformation under anhydrous conditions (Rubie and Ross 1994). Studies of the elasticity of hydrous wadsleyite and ringwoodite indicate that P- and S- wave velocities of the transition zone are consistent with the existence of hydrated wadsleyite and ringwoodite (Inoue et al. 2004; Jacobsen et al. 2004). These data indicate that a significant amount of water may be stored in the mantle especially in the transition zone.

Seismic discontinuities at 410 and 660 km depths are well established on a global scale to the point where they occur in reference velocity models such as PREM (Dziewonski and Anderson 1981). These discontinuities are usually attributed to the phase transformations of olivine in mantle peridotite. Olivine α-$(Mg,Fe)_2SiO_4$ transforms to wadsleyite β-$(Mg,Fe)_2SiO_4$ at a depth of approximately 410 km, and ringwoodite γ-$(Mg,Fe)_2SiO_4$ decomposes to perovskite $(Mg,Fe)SiO_3$ and magnesiowustite (Mg,Fe)O at approximately 660 km depth. The latter transformation is frequently termed the post-spinel transformation.

The topography and sharpness of these discontinuities depend on mantle temperatures, chemical compositions and mineral proportions (e.g., Agee 1998; Weidner and Wang 2000; Frost 2003). According to most seismological studies the 410 and 660 km discontinuities are sharp, and the change of density and velocity occurs over a small depth interval, 4-35 km for

1529-6466/06/0062-0017$05.00 DOI: 10.2138/rmg.2006.62.17

the 410 km discontinuity and <5 km for the 660 km discontinuity (e.g., Benz and Vidale 1993; Shearer 2000). Topography of the discontinuities has also been reported in seismic studies; i.e., elevations of 410 km and depression of 660 km in subduction zones and the opposite effects in hot mantle plume regions (e.g., Flanagan and Shearer 1998). Until recently these variations were believed to be consistent with the experimentally determined Clapeyron slopes of the olivine-wadsleyite and post-spinel transformations. For example, Ito and Takahashi (1989) reported a Clapeyron slope of −3.0 MPa/K, and Bina and Helffrich (1994) calculated a Clapeyron slope of −2.0 MPa/K for the post-spinel transformation. However, recent *in situ* X-ray diffraction studies of the post-spinel transformation in Mg_2SiO_4 and pyrolite compositions have implied a much gentler negative slope to this boundary (−0.4 to −1.3 MPa/K) (Katsura et al. 2003; Fei et al. 2004a; Litasov et al. 2005b) based on the newly established MgO and Au pressure scales (e.g., Speziale et al. 2001; Shim et al. 2002; Tsuchiya 2003). These results make it difficult to explain the topography of the 660 km discontinuity of about ±20 km (e.g., Gu et al. 1998) through thermal perturbations and indicate that the post-spinel phase transformation may account for less than a half of variations in depth of the 660 km discontinuity. Additional explanations for the observed topographic variations of the 660 km discontinuity are required and may reflect the influence of minor elements or volatiles.

In addition, two other phase transformations, which could be important in mantle dynamics and velocity structure of the Earth, are considered here: (1) the wadsleyite-ringwoodite transformation in peridotite, which is believed to be responsible for the seismic discontinuity at approximately 520 km (e.g., Shearer 1996), and (2) the post-garnet (garnet to perovskite) transformation in basalt (eclogite) composition (e.g., Ringwood 1994; Hirose et al. 1999; Litasov et al. 2004). The basaltic oceanic crust component of a subducting slab transforms to eclogite as the slab descends into the deep mantle. This basalt component may accumulate above 660 km due to a density crossover with peridotite mantle and it may create a complex velocity structure near the 660 km discontinuity (Ringwood 1994).

In this paper, we summarize recent studies on the effect of water on the location of phase boundaries and phase relations of mantle minerals. In addition, we examine the effect of water on the kinetics of these phase transformations. We also discuss the implications of these recent results with respect to seismic discontinuities and mantle dynamics.

RECENT PROGRESS ON PRESSURE SCALES FOR THE DETERMINATION OF PHASE BOUNDARIES IN MANTLE MINERALS

The boundaries of the phase transformations of mantle minerals were previously determined by the quenching technique (e.g., Ito and Takahashi 1989). The pressure scale in this technique is based on the calibration curve, i.e., the relation between the generated pressure and press load determined separately using pressure standards, which were determined by *in situ* X-ray diffraction technique. However, this procedure contains a large uncertainty due to the reproducibility of the experiments and unexpected temperature dependency of the generated pressure due to a different furnace assembly and starting materials. In order to overcome this difficulty, *in situ* X-ray diffraction techniques have been introduced. We can observe the reactions occurring in the samples at high pressure and temperature, and we can also measure the pressure values generated at high pressure and temperature by determination of the cell parameters of the standard materials such as Au, NaCl, and MgO. This technique has been used extensively by using intense X-ray from synchrotron radiation (e.g., Katsura et al. 2003).

An accurate pressure scale is essential for comparing the pressure of a phase boundary with the depth of a discontinuity in the mantle. A possible ambiguity in the use of Au as an *in situ* powder X-ray diffraction pressure scale was initially identified through the study of Irifune

et al. (1998) on the post-spinel phase boundary. Irifune et al. (1998) employed the equation of state (EOS) for Au of Anderson et al. (1989) to determine the pressure in their experiments from the unit cell parameters of Au measured *in situ*. Based on these data Irifune et al. (1998) proposed that the post spinel phase boundary occurred at a pressure that was approximately 2 GPa lower than that expected at the 660 km discontinuity. They suggested the possibility that a compositional change at the base of the transition zone may, therefore, cause the 660 km discontinuity, a possibility that was proposed by Ringwood (1994). Since this report of the inconsistency of the phase boundary with the 660 km discontinuity, attempts have been made to evaluate a number of pressure scales and to improve the scales at high pressure and temperature (e.g., Fei et al. 2004b).

Au, Pt, and MgO have been often used as pressure markers for *in situ* X-ray diffraction studies at high-pressure and temperature in the multianvil apparatus and in the diamond anvil cell (e.g., Fei et al. 2004b). It has been reported that the pressure scale of Au proposed by Anderson et al. (1989) underestimates the pressure at high temperatures due to incorrect evaluation of the thermal pressure (e.g., Matsui et al. 2000), although the Au pressure scale in general has a strong stress effect at low temperature. A pressure scale is essential for accurate determination of phase transformation boundaries and their Clapeyron slopes, however there is no consistency among the different pressure scales especially at pressures above 20 GPa at high temperature. For instance, the pressure differences calculated from the EOS of Au, Pt, and MgO (e.g., Jamieson et al. 1982; Anderson et al. 1989; Shim et al. 2002; Tsuchiya 2003) may be as large as 2.5 GPa at 25 GPa and 2000 K. Fei et al. (2004b) made a comprehensive review of different pressure scales and calibrated the Au and Pt scales based on the MgO EOS (Speziale et al. 2001).

Based on the above studies on the pressure scale, the equation of state of MgO is now considered to be one of the most reliable pressure scales at high pressure and temperature, since there are many reliable shock compression, elasticity, and static compression data at high pressure and temperature. The Au pressure scale was also improved by Shim et al. (2002) by using the new reliable compression data of Au. Fei et al. (2004b) made a correction of the Au pressure scale by Shim to fit the MgO pressure scale by Speziale et al. (2001). Tsuchiya (2003) presented a Au pressure scale based on molecular dynamic calculations, and it is generally consistent with that of the Au pressure scale by Fei et al. (2004b) and the MgO pressure scale by Speziale et al. (2001). Thus, we adopt the pressure scale at high temperature based on the unit cell volume of Au using EOS by Tsuchiya (2003) and MgO using EOS by Speziale et al. (2001) in the present review. We found that, the pressures calculated by the MgO scale by Speziale et al. (2001) are generally consistent with those by Au scale by Tsuchiya (2003). We estimated that P (MgO; Speziale et al. 2001) − P (Au; Tsuchiya 2003) = 0.08 ± 0.36 GPa in the pressure range of 20-25 GPa and temperatures between 1500 and 2200 K. However, at lower temperatures of 1200-1500 K the pressure difference may exceed 0.4 GPa (Litasov et al. 2006). The MgO pressure scale proposed by Matsui et al. (2000) is also used in some studies (e.g., Katsura et al. 2004). This pressure scale gives the pressures generally 0.1 GPa lower than those of the MgO scale by Speziale et al. (2001).

It is noteworthy that there are several other uncertainties in determination of the phase boundaries, such as the effect of pressure on Electromotive force (EMF), stress differences in sample and standard, and kinetics of the phase transformation. We can minimize the stress differences in the sample and standard by annealing at high pressure and temperature and by placing them in different parts in the furnace assembly. We can also minimize the effect of the reaction kinetics by conducting reversal runs in the *in situ* X-ray diffraction experiments. However, the most serious problem is the effect of pressure on EMF. The current temperature values without pressure correction for EMF is likely to be underestimated by several tens degrees based on previous estimates (e.g., Ohtani 1979).

EFFECT OF WATER ON PHASE TRANSFORMATION

Dry and wet phase boundaries in the olivine-wadsleyite transformation

Water may modify the location of the olivine-wadsleyite transformation boundary as a result of the difference in water solubility between olivine and wadsleyite. At 1300-1500 K wadsleyite contains 5-40 times more water than olivine (e.g., Kohlstedt et al. 1996; Chen et al. 2002), therefore the phase transition boundary can be shifted to lower pressures by the addition of water. The water content in olivine is usually determined by Fourier Transform Infrared Spectroscopy (FTIR) (Paterson et al. 1982) or Secondary Ion Mass Spectrometry (SIMS) (e.g., Kurosawa et al. 1997; Demouchy et al. 2005). Water content is estimated by the integrated intensity of the OH absorption band of FTIR measurement based on the method by Paterson et al. (1982). Recently, the FTIR calibration of Paterson et al. (1982) for the water content in olivine has been reexamined and shown to be about three times as large as those of the previous values (Bell et al. 2003). If we adopt the new calibration, the partition coefficients of water between wadsleyite and olivine at 1300-1500 K range become one third of the previous value, i.e., 1.6-13. However, we need more detailed studies of the water contents in wadsleyite using SIMS and improving the Paterson's calibration for wadsleyite. Demouchy et al. (2005) provided extensive SIMS data for water content in wadsleyite.

The olivine-wadsleyite transformation has been intensively studied both under anhydrous and hydrous conditions and the results are summarized in Figure 1. Katsura and Ito (1989) determined that the Clapeyron slope of the olivine-wadsleyite phase boundary is 2.5 MPa/K and the pressure interval of the olivine-wadsleyite transformation loop for $(Mg,Fe)_2SiO_4$ of Fo_{90} composition is 0.5 GPa at 1900 K. Akaogi et al. (1989) calculated the olivine-wadsleyite phase boundary using calorimetric data, and they suggested a shallower Clapeyron slope of 1.5±0.5 MPa/K, and Bina and Helffrich (1994) recalculated the data by Akaogi et al. (1989) and obtained a Clapeyron slope of 3.0 MPa/K. Recent *in situ* X-ray diffraction studies have shown that the Clapeyron slope is 3.6 MPa/K (Morishima et al. 1994) to 4.0 MPa/K (Katsura et al. 2004) in Mg_2SiO_4 and Fo_{90} systems. Katsura et al. (2004) estimated that the width of the binary loops of the phase transformation is about 0.4 GPa at 1900 K and about 0.6 GPa at 1600 K for Fo_{90}.

Litasov et al. (2006) performed preliminary experiments to determine the olivine-wadsleyite transformation in anhydrous and hydrous pyrolite compositions using *in situ* X-ray diffraction (Fig. 1). Although the Clapeyron slope of the boundary was not determined precisely, it was

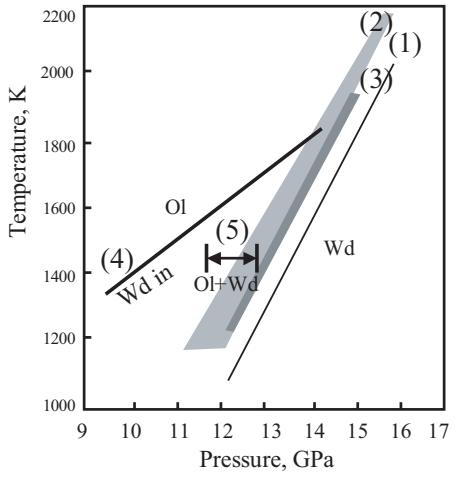

Figure 1. Comparison of the olivine-wadsleyite transformation boundaries obtained by different studies (Litasov et al. 2006). (1), olivine-wadsleyite boundary in Mg_2SiO_4 by Morishima et al. (1994); (2), Fo_{90} by Katsura et al. (2004) under the dry conditions. (3), the phase boundary of pyrolite under the dry conditions (Litasov et al. 2006). (4), the phase boundary of pyrolite under the hydrous conditions (3.0 wt% H_2O) (Litasov et al. 2006). (5), Chen et al. (2002). Ol, olivine; Wd, wadsleyite. Pressure was calculated based on the pressure scale of Tsuchiya (2003). Preliminary experiments by Litasov et al. (2006) indicate the field of olivine + wadsleyite broadens under the wet conditions.

found to be consistent with the slope in $(Mg,Fe)_2SiO_4$ determined by Katsura et al. (2004) under dry conditions. Using the Clapeyron slope of Katsura et al. (2004) and the Au pressure scale by Tsuchiya (2003), we can obtain a linear equation for the olivine-wadsleyite boundary in pyrolite under dry conditions, which is P (GPa) = 0.0039 T (K) + 7.47. The choice of pressure scale does not significantly affect the slope of the phase transformation. The pressure interval of olivine and wadsleyite coexistence is about 0.2-0.3 GPa in these experiments.

Several experimental and theoretical studies on the effect of water on the olivine-wadsleyite phase transformation and water partitioning between olivine and wadsleyite have been carried out to date. Wood (1995) argued that hydrogen, being more soluble in wadsleyite than olivine, expands the stability field of wadsleyite to lower pressures due to the effect of hydrogen on the configuration entropy of disorder in wadsleyite. Wood (1995) calculated that the presence of 500 ppm H_2O in olivine would expand the olivine-wadsleyite loop interval from 7 km for the anhydrous system to about 22 km for the hydrous system. Smyth and Frost (2002), on the other hand, experimentally observed a shift of the olivine-wadsleyite phase boundary by about 1 GPa to lower pressures using $Fo_{92\text{-}98}$ and the peridotite composition with Fo_{89} olivine both containing 3 wt% H_2O. This result is consistent with that of Litasov et al. (2006) determined by *in situ* X-ray diffraction experiments. Chen et al. (2002) also determined the olivine-wadsleyite phase transformation boundary in Fo_{100} and Fo_{90} under dry and hydrous conditions by heating both dry and hydrous (11 wt% H_2O) charges simultaneously at 1473 K and 12.6-14.7 GPa (Fig. 1). They also observed a shift of the olivine-wadsleyite phase boundary to lower pressure, but found a decrease of the pressure interval of the olivine-wadsleyite loop to 0.3 GPa.

Wadsleyite-ringwoodite transformation

The data for the determination of the wadsleyite-ringwoodite phase boundary are limited compared to those for the olivine-wadsleyite and the post-spinel phase boundaries in the olivine and peridotite systems. The wadsleyite-ringwoodite phase boundary in $(Mg,Fe)_2SiO_4$ determined using quenching experiments (Katsura and Ito 1989) has a significant positive Clapeyron slope of +5 MPa/K. Suzuki et al. (2000) reported a linear equation expressed as P (GPa) = 0.0069 T (K) + 8.43 for the phase boundary in Mg_2SiO_4 using the NaCl pressure scale (Brown 1999). Litasov and Ohtani (2003) observed a minor shift of the boundary to higher pressure in the CMAS-pyrolite system with 2 wt% H_2O, whereas Kawamoto (2004) observed wadsleyite at 20 GPa and 1573 K in pyrolite with 13 wt% H_2O, which suggests a shift of the phase boundary by 2.5 GPa to higher pressures compared to that observed in the anhydrous system. Inoue et al. (2001) also showed a shift of the phase boundary in $Fo_{80\text{-}100}$ with 1 wt% H_2O, which is consistent with the results described above, although the exact shift in pressure of the boundary has not yet been reported.

There are no data on the effect of water on the width of the wadsleyite-ringwoodite transformation interval. Katsura and Ito (1989) determined the pressure interval of the wadsleyite-ringwoodite loop to be ~0.9 GPa (24 km) for anhydrous Fo_{90} at 1473-1873 K, whereas Frost (2003) calculated that it may be reduced to ~0.7 GPa (20 km) in a garnet peridotite. The cause of the shift of the phase boundary under water saturated conditions is not clear. It might be caused by the lower solubility of water in ringwoodite relative to wadsleyite, which is suggested by the data on the maximum water solubilities of these phases; i.e., the maximum water solubility in ringwoodite (2.6 wt%) is lower than that in wadsleyite (3.4 wt%) (e.g., Kohlstedt et al. 1996; Inoue et al. 1998).

Post-spinel transformation

In Figures 2(A) and (B) we summarize recent studies on the determination of the post-spinel phase boundary in Mg_2SiO_4 and peridotite under dry conditions using both the multianvil

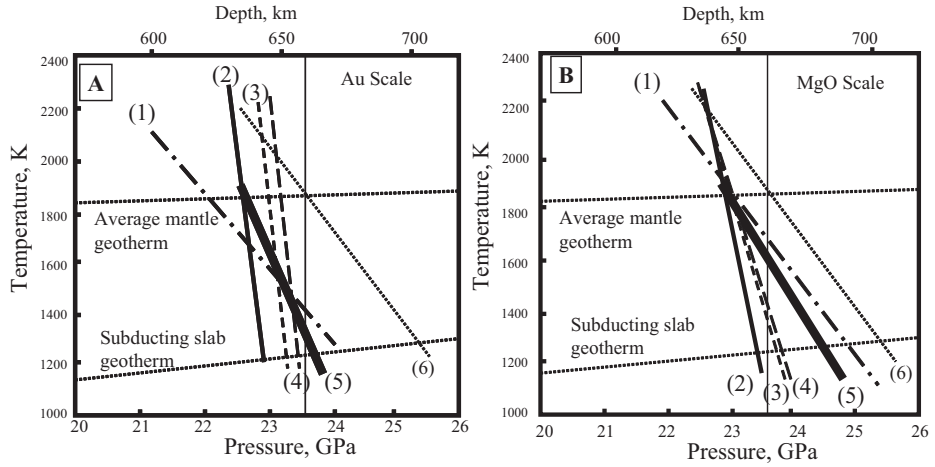

Figure 2. Comparison between post-spinel transformation boundaries determined by different studies using (A) the Au pressure scale of Tsuchiya (2003) and (B) the MgO pressure scale of Speziale et al. (2001). The average mantle geotherm is after Akaogi et al. (1989). The cold subduction geotherm is after Kirby et al. (1996). (1) the phase boundary in $(Mg,Fe)_2SiO_4$ determined by the quenching method by Ito and Takahashi (1989). This boundary was determined by the pressure scale using some phase boundaries determined based on the Au scale by Jamieson et al.(1982) as pressure fixed points. We corrected this Au pressure scale to new scales of Au (Tsuchiya 2003) and MgO (Speziale et al. 2001). (2) the boundary in pyrolite (Litasov et al. 2005b) under dry conditions. (3), (4) the boundary in Mg_2SiO_4 under dry conditions determined by Katsura et al. (2003) and Fei et al. (2004a), respectively. (5) the post-spinel phase boundary in hydrous pyrolite (Litasov et al. 2005a). (6) the phase boundary in Mg_2SiO_4 determined by diamond anvil cell (Shim et al. 2001).

press and diamond anvil cell. Most studies made by *in situ* X-ray diffraction study using the multianvil press indicate that the post-spinel phase boundary is lower than that expected for the depth of the 660 km discontinuity (Figs. 2A,B).

Experiments made using the diamond-anvil cell (DAC) (Chudinovskih and Boehler 2001; Shim et al. 2001) and those made with the multi-anvil press with an improved technique by taking into account of kinetics based on following reliable pressure scales (Katsura et al. 2003; Fei et al. 2004a; Litasov et al. 2005b) have shown the pressure of the phase boundary under dry conditions to be in closer agreement with conditions at the 660 km discontinuity (Figs. 2A,B). The post-spinel phase boundary of Mg_2SiO_4 determined by Fei et al. (2004a) using the MgO pressure scale of Speziale et al. (2001) is consistent with the depth of the 660 km discontinuity, i.e., $\Delta P_{660} = (P_{660\,km} - P_{measured}$ at 1850 K) = 0.6 GPa. Litasov et al. (2005b) reported $\Delta P_{660} = 1.0$ GPa using the Au scale of Tsuchiya (2003) for anhydrous pyrolite. Ignorance of the pressure effect on thermocouple Electromotive force (EMF) in multianvil experiments underestimates temperatures (e.g., Ohtani 1979), and it further reduces discrepancy. The results obtained by Chudinovskikh and Boehler (2001) for Mg_2SiO_4 using the DAC are consistent with the data of Fei et al. (2004a). The data determined by Shim et al. (2001) using the DAC indicate that the post-spinel transformation boundary (Figs. 2A,B) is close to the depth of the 660 km seismic discontinuity. The results obtained by DAC, however, have a large temperature (100-200 K) uncertainty. DAC results are also relatively scattered, causing a high uncertainty in the estimation of the Clapeyron slope of the phase boundary.

It should be noted that the most remarkable results of the recent *in situ* X-ray diffraction experiments are the gentle slope of the phase boundary, i.e., previous results of the Clapeyron slope, dP/dT , were relatively large around 2 MPa/K (Ito and Takahashi 1989; Irifune et al.

1998), whereas Katsura et al. (2003), Fei et al. (2004a) and Litasov et al. (2005b) indicate that the slope is small and approximately 0.4~1 MPa/K. The improvement for determination of the equilibrium boundary especially at temperatures below 1500 K has been made in the recent *in situ* study, i.e., there is a possibility that the old data overestimated the pressure of the phase transformation due to a slow transformation kinetics at low temperature (e.g., Kubo et al. 2002a). Effect of slow transformation kinetics was overcome by observation of forward and reversal reactions by changing pressure at a constant high temperature (e.g., Katsura et al. 2003; Litasov et al. 2005b). A small Clapeyron slope of the post-spinel transformation has very important implications for the 660 km discontinuity as discussed below in detail; the dry Clapeyron slope cannot explain the topography of the 660 km discontinuity of about ±20 km (e.g., Gu et al. 1998).

Litasov et al. (2006) determined the phase boundary by *in situ* X-ray diffraction study in the pressure range of 20-26 GPa and temperatures up to 2300 K. The post-spinel phase boundary defined by a boundary of the appearance of Mg-perovskite can be expressed as P (GPa) = −0.0005 T (K) + 23.54 using the Au pressure scale by Tsuchiya (2003) and P (GPa) = −0.0008 T (K) + 24.42 using the MgO pressure scale by Speziale et al. (2001) (see Figs. 2 and 3).

Ito and Takahashi (1989) reported that the pressure interval of coexisting ringwoodite and Mg-perovskite + magnesiowustite to be less than 0.1 GPa for $(Mg_{0.9}Fe_{0.1})_2SiO_4$ based on quench experiments. On the other hand, Hirose (2002) and Nishiyama et al. (2004) reported a relatively wide pressure interval (0.5-0.7 GPa) for the post-spinel transformation in pyrolite. Litasov et al. (2005b) reported a narrow pressure interval of coexistence of 0.1-0.5 GPa based on their *in situ* X-ray diffraction study on anhydrous pyrolite.

In a water bearing system, a shift of the post-spinel phase boundary to higher pressure may be expected due to the difference in the water solubility between ringwoodite and Mg-perovskite + magnesiowustite assemblages. Ringwoodite can contain H_2O up to 2.6 wt% at 1100 °C and 20 GPa (Kohlstedt et al. 1996; Inoue et al. 1998), whereas Mg-perovskite and magnesiowustite contain very limited amounts of H_2O (<30 and <100 ppm, respectively)(Bolfan-Casanova et al. 2000; 2002; 2003; Litasov et al. 2003).

Higo et al. (2001) studied the influence of water on the phase boundary of the Mg_2SiO_4 post-spinel phase transformation and reported a shift of 0.2 GPa to higher pressure at 1873 K. However, the effect of water has not been studied in detail. Recently, Litasov et al.

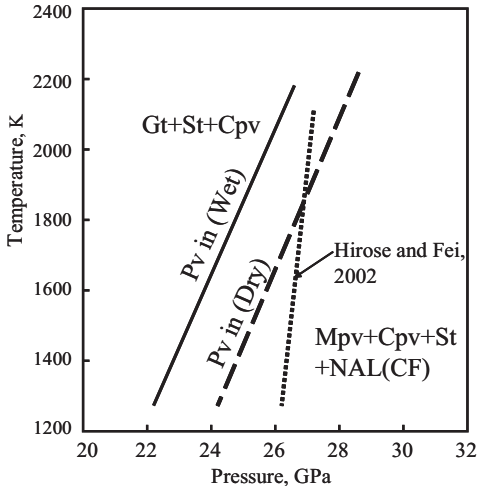

Figure 3. Comparison of garnet-perovskite phase boundaries in basalt (MORB) under dry and wet conditions. The dashed line (Litasov et al. 2004) and solid line (Sano et al. 2006) show the first appearance of perovskite determined by *in situ* X-ray diffraction experiments using pressures calculated based on the Au pressure scale of Tsuchiya (2003). The phase boundary determined using quench experiments by Hirose and Fei (2002) is shown as a dotted line. Gt, garnet; St, stishovite; Cpv, Ca-perovskite; Mpv, Mg-perovskite; NAL, Na-Al hexagonal phase; CF, aluminous orthorhombic phase with Ca-ferrite structure.

(2005a) made a detailed determination of the post-spinel phase boundary with a hydrous pyrolite composition with 2.0 wt% H_2O using *in situ* X-ray diffraction at high pressure and temperature. The pressure of the post-spinel transformation boundary in a hydrous pyrolite composition was found to be higher by about 0.6 GPa than that of anhydrous pyrolite at 1473 K, whereas there is no obvious difference in pressure of this boundary at higher temperatures (1773-1873 K). The phase boundary defined by the appearance of Mg-perovskite can be expressed as P (GPa) = −0.002 T (K) + 26.3 in the temperature range from 1000 to 1800 K for pyrolite containing 2.0 wt% H_2O. Superhydrous phase B coexists both with ringwoodite and Mg-perovskite in hydrous runs made below 1500 K.

It should be noted that the Clapeyron slope of the phase boundary is −2 MPa/K in pyrolite containing 2.0 wt% H_2O which is greater than that observed under dry conditions. A large Clapeyron slope is consistent with the temperature dependency of the H_2O solubility in ringwoodite, i.e., its H_2O content is about 2.0 wt% at around 1200 K, whereas it decreases to about 0.5 wt% at 1700 K (Ohtani et al. 2001). Since the shift of the phase boundary can be related to the water content of ringwoodite, a large amount of the pressure shift can be expected at lower temperature and a smaller shift at relatively higher temperature, resulting in a large Clapeyron slope of the phase boundary.

Based on the results of *in situ* X-ray diffraction experiments of the post-spinel transformation in anhydrous and hydrous pyrolite we may conclude that both pyrolite and Mg_2SiO_4 show smaller negative Clapeyron slopes for the post-spinel phase boundary between −0.4 and −1.0 MPa/K using both Au and MgO pressure scales (Speziale et al. 2001; Tsuchiya 2003), whereas the addition of 2.0 wt% H_2O may shift the boundary to higher pressures by ~0.6 GPa (15 km) at 1473 K and produce a larger Clapeyron slope of about –2 MPa/K. The change of the Clapeyron slope has important implications for slab dynamics since it affects the magnitude of the buoyancy force operating in slabs. The topography of the 660 km discontinuity may be at least partly due to the water content in the slabs.

Post-garnet transformation in basalt (MORB)

The post-garnet transformation has a positive Clapeyron slope, and it occurs at higher pressure than the decomposition of ringwoodite in peridotite compositions under dry condition [e.g., Kubo and Akaogi 2000]. Based on quench experiments, Hirose and Fei (2002) demonstrated that the post-garnet phase transformation in basalt occurs at 27 GPa and 1900 K with a slightly positive Clapeyron slope (dP/dT = +0.8 MPa/K) as shown in Figure 3. Using *in situ* X-ray diffraction, Oguri et al. (2000) determined the post-garnet transformation boundary in natural pyrope at 25 GPa and 1900 K with a significant positive dP/dT (+6.4 MPa). On the other hand, Litasov et al. (2004) made an *in situ* X-ray diffraction study of the phase transformation in basalt under dry conditions, and showed that their data are inconsistent with the previous quench experiments by Hirose and Fei (2002), possibly due to corrections for the thermal pressure resulting in a large positive dP/dT of the post-garnet transformation in basalt (+4.1 MPa/K). The experiments by Litasov et al. (2004) revealed that the post-garnet phase boundary is expressed as P (GPa) = 0.0046 T (K) + 18.40 using the Au pressure scale by Tsuchiya (2003) as shown in Figure 4. The pressure interval of coexistence of garnet and Mg-perovskite is very narrow and less than 0.5 GPa.

Using quench experiments, Litasov and Ohtani (2005) observed a shift in the post-garnet transformation boundary in basalt by ~1 GPa to lower pressure with the addition of 2 wt% H_2O. Sano et al. (2006) confirmed an approximate 2 GPa shift of the phase boundary under wet conditions (~10 wt% H_2O) using *in situ* X-ray diffraction. They observed a CaMg-perovskite bearing assemblage at temperatures below 1400 K. At 1400-1500 K they observed the transformation of Mg-perovskite to garnet and the reversal transformation at about 22.9-23.1 GPa (Fig. 5). The resulting equation for the post garnet transformation in hydrous basalt can be expressed as P (GPa) = 0.0049 T (K) + 15.94 using the Au pressure scale by Tsuchiya (2003).

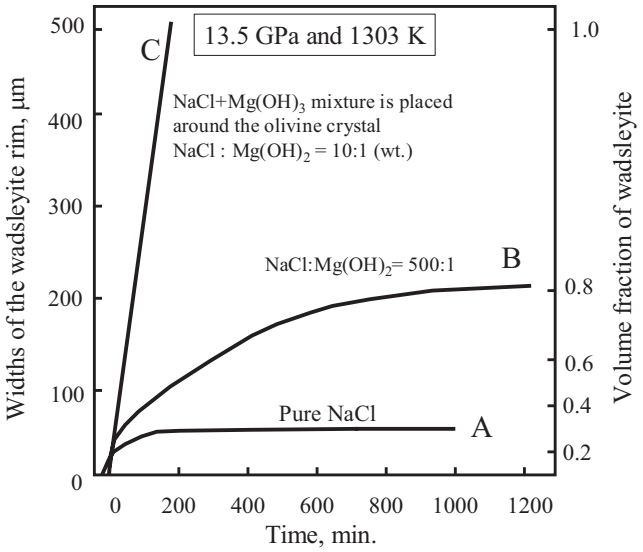

Figure 4. The time dependence of the width and volume fraction of a wadsleyite rim growing on a single crystal of San Carlos olivine under dry and wet conditions at 13.5 GPa and 1303 K. Details are given in Kubo et al. (1998). Water was added as brucite $Mg(OH)_2$ and its content was controlled by the ratio of NaCl and brucite surrounding the single crystal sample. (A) dry condition; (B) 500:1 mixture of NaCl and brucite; (C) 10:1 mixture (weight) of NaCl and brucite. The transformation is clearly enhanced by water.

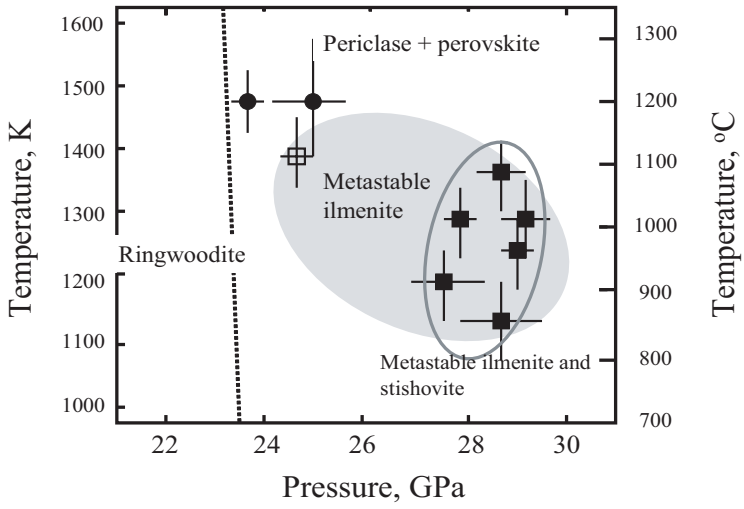

Figure 5. Pressure-temperature diagram showing the conditions where metastable assemblages were observed in experiments on the post-spinel transformation (see Kubo et al. 2002a). The dotted line is the equilibrium boundary between Mg_2SiO_4 ringwoodite and $MgSiO_3$ perovskite + MgO periclase. The conditions where metastable assemblages appear are also shown. Solid circles, ilmenite and stishovite do not appear but stable assemblage of perovskite and periclase appears; open square, ilmenite + periclase assemblage appears; solid squares, both ilmenite + periclase and stishovite + periclase assemblages appear.

The shift of the post garnet phase boundary to lower pressure cannot be explained by the effect of water solubility in the coexisting phases. Majorite garnet contains water up to 1130-1250 ppm H_2O, (Katayama et al. 2003) which is larger than Mg-perovskite (<30 ppm; Litasov et al. 2003; Bolfan-Casanova et al. 2003). Thus a shift of the phase boundary to higher pressure might be expected. Stishovite may contain a significant amount of water (up to 1500 ppm as reported by Chung and Kagi 2002), but it exists in both the garnet- and perovskite-bearing assemblage. The effects of the other phases such as Al-rich NAL phase and Ca-perovskite are not clear.

Litasov et al. (2005a) suggested a change in the oxidation state in the hydrous fluid phase under wet conditions causes the shift of the boundary due to a change in ferric iron content in Mg-perovskite. Since aluminous Mg-perovskite can contain a significantly higher amount of Fe^{3+} (McCammon 1997), the difference in the oxidation state causes a different ferric iron content in Mg-perovskite. We observed a difference in the iron content in Mg-perovskite under the dry and wet conditions (Litasov et al. 2005a; Sano et al. 2006) perhaps due to such a change of ferric iron content in Mg-perovskite. Another explanation is that the fluid can dissolve the major elements such as Mg, Si and Fe (e.g., Kawamoto et al. 2004), and thus it can change the composition of minerals, resulting in the shift of the location of the phase boundary (Sano et al. 2006).

EFFECT OF WATER ON PHASE TRANSFORMATION KINETICS

Olivine-wadsleyite phase transformation kinetics

Water plays an important role in controlling rheological properties of the mantle, since a trace amount of water lowers the strength of olivine crystals, i.e., hydrolytic weakening (e.g., Karato 1989). Olivine-wadsleyite transformation kinetics has been studied by various authors under dry conditions (e.g., Mosenfelder et al. 2001; Kerschhofer et al. 2000). However, the effect of water on the transformation kinetics has not been studied so much, although water may affect the phase transformation kinetics of mantle minerals. Recently, Kubo et al. (1998) and Hosoya et al. (2005) have conducted experiments to study the effect of water on the kinetics of the olivine-wadsleyite transformation based on both quench experiments using olivine single crystals and *in situ* X-ray diffraction experiments of polycrystalline olivine

Kubo et al. (1998) showed an enhancement of the transformation rate by water based on quench experiments using single crystals of San Carlos olivine that transformed to wadsleyite. The growth rate is roughly estimated from the thickness of the wadsleyite rim on the olivine single crystals. Figure 4 shows the time dependence of the width and volume fraction of wadsleyite rim under the dry and wet conditions. In dry runs, wadsleyite growth was retarded with time and eventually ceased after several hundred minutes as shown in Figure 4. Whereas, in wet runs, the wadsleyite grew more rapidly compared to the dry runs, resulting in a difference in growth rate between dry and wet conditions. These experiments clearly indicate that the growth rate of the wadsleyite rim was enhanced by the presence of water.

The volume change associated with the transformation is often large in solid-state first order transformations, resulting in the development of localized stress (e.g., Rubie and Thompson 1985). In dry runs, a localized pressure drop in the relict olivine as a result of the volume change during the transformation possibly causes a decrease in the free energy change of the reaction, resulting in a decrease in the growth rate (Liu et al. 1998). Plastic flow of the outer rim can relax the localized pressure drop and thus controls the growth rate of the wadsleyite rim, whereas a localized pressure drop in olivine may be relaxed perhaps due to water weakening in wet runs. Thus, wadsleyite grows more rapidly compared to the dry runs, resulting in the difference in growth rate between dry and wet conditions. Figure 4 clearly implies that a small amount of water, about 0.12–0.5 wt%, enhances the olivine-wadsleyite phase transformation kinetics corresponding roughly to a temperature increase of about 150 degrees.

Kubo et al. (2004) and Hosoya et al, (2005) studied the effect of water on the phase transformation kinetics by *in situ* X-ray diffraction using the multianvil press, SPEED1500 at beam line BL04B1 of Spring 8 of Japan Synchrotron Research Institute. They obtained growth rate data at 13.4-15.8 GPa, 730-1100 °C, for 660-5000 ppm weight H_2O to determine the pressure, temperature and water content dependences on the growth kinetics of the α-β transformation of Mg_2SiO_4. The growth in the polymorphic transformation is controlled by interface kinetics (Turnbull 1956). The growth rate as a function of pressure, temperature and water content can be described as follows, where A is a pre-exponential factor, T is absolute temperature, C_{OH} is water content in ppm by weight, n is the water content exponent, ΔH_a is the activation enthalpy for growth, P is pressure, V^* is the activation volume for growth, R is the gas constant, and ΔGr is the free energy change of the transformation. This rate equation was fitted to the growth rate data by a weighted least-squares procedure, which yields $\ln A = -18.0 \pm 3.8$ ms^{-1} wt. ppm $H_2O^{-3.2}$, $n = 3.2 \pm 0.6$, $\Delta H_a = 274 \pm 87$ kJ/mol, and $V^* = 3.3 \pm 3.8$ cm^3/mol. Results of the fitting of the pressure, temperature, and water content against the growth rate are shown in Figure 6. This study demonstrates that water greatly enhances the growth rate at the olivine transformation. Because the depth of the olivine transformation in cold slabs is controlled by the growth kinetics (Rubie and Ross 1994), the effect of water on the growth kinetics must be considered when estimating fields of olivine metastability.

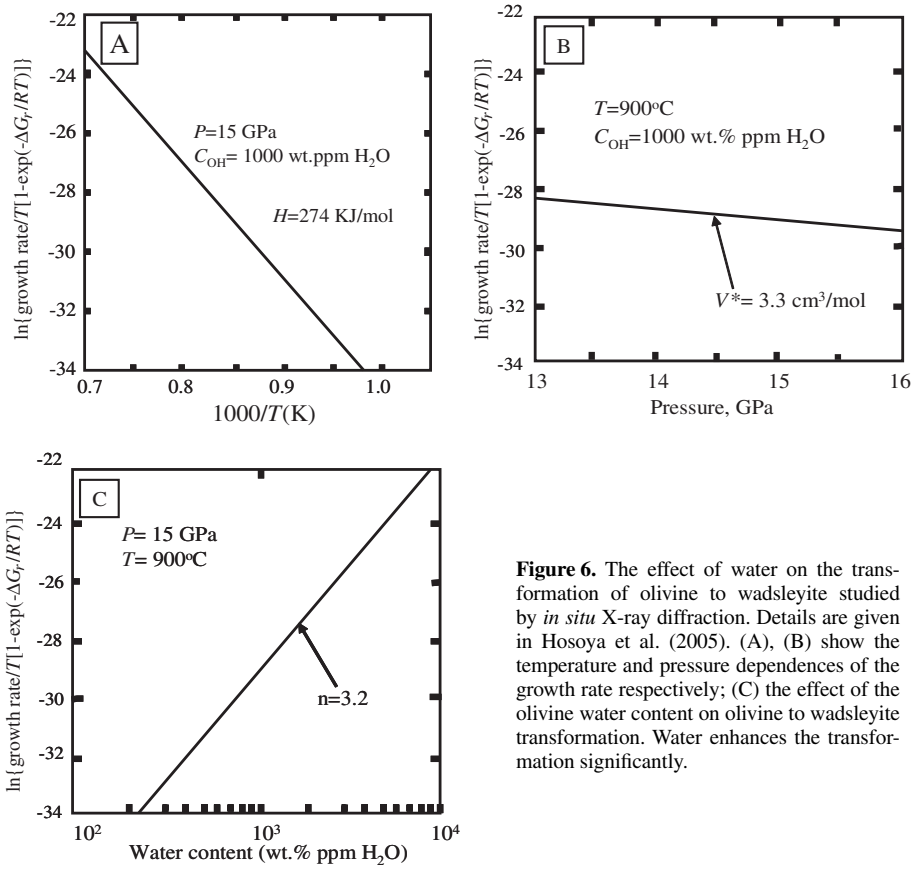

Figure 6. The effect of water on the transformation of olivine to wadsleyite studied by *in situ* X-ray diffraction. Details are given in Hosoya et al. (2005). (A), (B) show the temperature and pressure dependences of the growth rate respectively; (C) the effect of the olivine water content on olivine to wadsleyite transformation. Water enhances the transformation significantly.

Post-spinel and post garnet phase transformation kinetics

Kinetics of the post-spinel and post-garnet transformations have been studied by Kubo et al. (2002a,b) under dry conditions. Kubo et al. (2002a) showed that a metastable phase assemblage is observed at low temperatures in the initial stage of the post-spinel transformation. They observed decomposition of ringwoodite to periclase + stishovite or periclase + akimotoite ($MgSiO_3$). These assemblages formed in the initial stage of the phase transformation but disappeared after a few minutes, which indicates that these assemblages are metastable. The pressure and temperature conditions of appearance of the metastable assemblage are shown in Figure 5. These observations suggest that a metastable assemblage such as periclase + stishovite or periclase + akimotoite ($MgSiO_3$) might exist in dry and cold subducting slabs.

Kubo et al. (2002b) clarified that post-garnet transformation kinetics are very sluggish, and we can expect a metastable garnetite layer in the lower mantle due to low temperatures of the penetrating slabs. Figure 7 shows clearly that the post-garnet transformation is remarkably sluggish compared to the olivine-wadsleyite and post-spinel transformations. The appearance of a metastable assemblage in the post-spinel transformation might cause a relatively fast reaction rate of the transformation.

The effect of water on the transformation kinetics in the post-spinel and post-garnet transformations has not yet been studied. However, it might be evaluated qualitatively based on the *in situ* X-ray diffraction study at high pressure and high temperature (Litasov et al. 2004, 2005a,b; Sano et al. 2006). Litasov et al. (2005b) observed the phase transformation from ringwoodite to magnesiowustite and Mg-perovskite proceeds at 1623 K within 30 minutes. On the other hand, Litasov et al. (2005a) observed that a similar reaction rate in peridotite plus 2.0 wt% water at 1423 K. These results suggest that water (about 2.0 wt%) can enhance reaction rates to a degree that may be equivalent to a temperature increase of about 200 K.

In situ X-ray diffraction studies of the post garnet transformation of basalt under dry and wet conditions indicate that the transformation at 1473 K proceeds within 30 minutes under

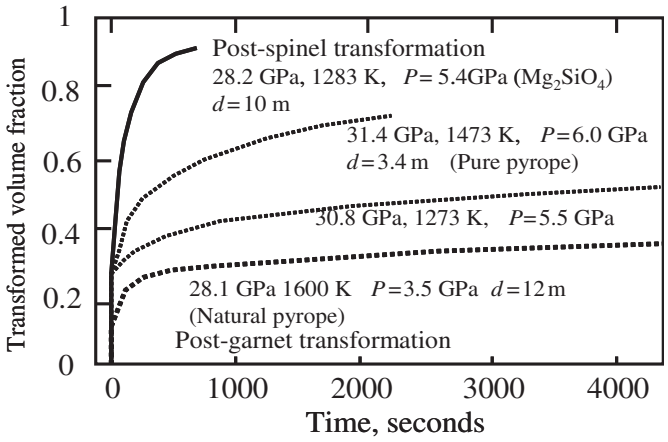

Figure 7. The rate of the post-spinel and post-garnet transformations after Kubo et al. (2002a,b). The solid curve indicates the rate of the post-spinel transformation of Mg_2SiO_4 at 28.2 GPa and 1283 K. The thin dotted curves are the rate of the post-garnet transformation in $Mg_3Al_2Si_3O_{12}$ at 31.4 GPa and 1473 K and 30.8 GPa and 1273 K. A thick dotted curve is the rate of the post-garnet transformation in natural pyropic garnet $(Mg_{0.724}Fe_{0.184}Ca_{0.111})_3(Al_{0.872}Cr_{0.0044}Ti_{0.010})_2Si_{3.064}O_{12}$. The rate of the post-spinel transformation is significantly faster than that of the post-garnet transformation. ΔP, overpressure (a pressure interval from the equilibrium boundary): d, grain size of the sample.

the wet conditions (Sano et al. 2006), whereas the temperature has to be raised to 1973 K for the same reaction time scale under dry conditions (Litasov et al. 2004). Water enhances the post-garnet transformation kinetics similar to the post-spinel transformation kinetics, although the reaction rate in the post-garnet transformation is sluggish compared to the post-spinel phase transformation. Although our preliminary studies suggest that both post-spinel and post-garnet transformation kinetics are enhanced by water, we need more quantitative studies by in situ X-ray diffraction on the reaction under wet conditions to quantify the effect of water.

IMPLICATION FOR SEISMIC DISCONTINUITIES AND PHASE TRANSFORMATION BOUNDARIES UNDER DRY AND WET CONDITIONS

410 km seismic discontinuity and olivine-wadsleyite phase boundary

The 410 km seismic discontinuity is considered to be caused by the transformation from olivine to wadsleyite in peridotite mantle. The average depth of the discontinuity is 411 km (Gu et al. 1998) and 418 km (Flanagan and Shearer 1998, 1999) using stacking SS and PP precursors. Figure 8 summarizes the shifts of the phase boundaries in the mantle as a result of the addition of water. Katsura et al. (2004) estimated the mean temperature at the 410 km seismic discontinuity to be 1760 ± 45 K for pyrolite mantle using the average depth of

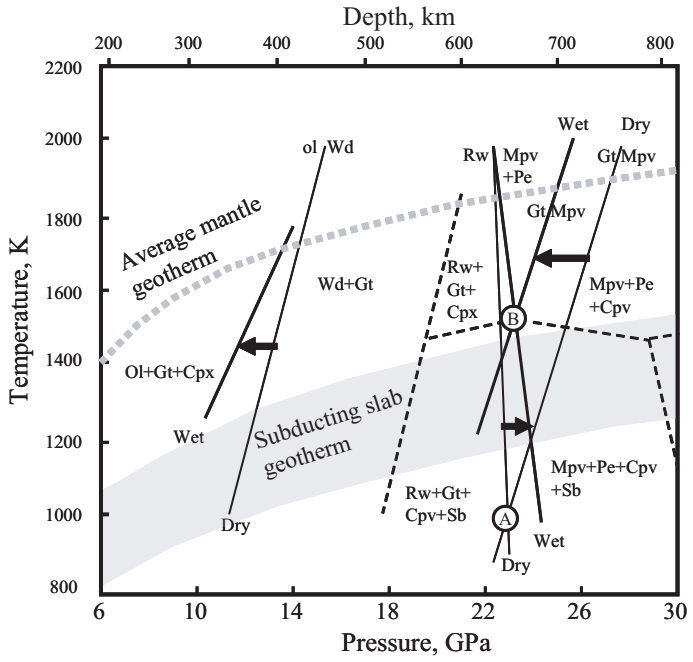

Figure 8. Phase boundaries in peridotite and basalt under dry and wet conditions. The stability fields of wasleyite and ringwoodite expand under wet conditions at low temperatures (Litasov et al. 2005a,b), whereas the post garnet transformation shifts to lower pressures under wet conditions (Litasov et al. 2004; Sano et al. 2006). The grey dotted curve is the average temperature of the mantle (Akaogi et al. 1989). The shaded area represents the temperature range of the slabs (Kirby et al. 1996). The phase boundaries of the post-spinel and post-garnet transformations cross at around 1000 K (A) under dry conditions and 1400 K (B) under wet conditions. Rw, ringwoodite; Sb, superhydrous phase B; Pe, periclase. The other abbreviations are the same as those given in Figures 1 and 3.

the discontinuity. As discussed in the previous section, the existence of water in the mantle (~1760 K) may elevate the depth of the 410 km discontinuity by a few kilometers.

Global topography of the 410 km seismic discontinuity indicates depth variations of approximately ±20 km (Flanagan and Shearer 1998). Local seismological studies indicate greater depth variations in some areas. For example, the maximum elevation of the discontinuity in subduction zones is around 60-70 km, which is consistent with a temperature anomaly of about 1000 K if we apply the Clapeyron slope of the olivine-wadsleyite phase boundary of +3~4 MPa/K (e.g., Collier et al. 2001). Such a temperature anomaly of 1000 K at the 410 km discontinuity is too large given that the normal temperature of the discontinuity is around 1760 K based on the geotherm estimated by some authors (e.g., Akaogi et al. 1989; Katsura et al. 2004). Since water and temperature have a similar effect on the phase boundary, the topography of the 410 km seismic discontinuity in some regions may be also explained by the presence of water in subduction zones, i.e., some fraction of the topography of the discontinuity may be explained by the effect of water in combination with the temperature effect as shown in Figure 8.

The width of the 410 km discontinuity varies from 4 to 35 km (Shearer 2000). The phase relations in the olivine composition in peridotite indicate a width of the binary loop of coexistence of olivine and wasleyite is 25 km at 1473 K and 14 km at 1873 K (Katsura and Ito 1989). Frost (2003) reviewed recent experimental and thermodynamic data on the olivine-wadsleyite transformation and discussed the possibility of a 4-6 km width, i.e., the minimum of the range of the width of discontinuity. Frost (2003) found this width to be consistent with the olivine-wadsleyite phase transformation in a peridotite composition containing garnet and pyroxenes, which makes the phase boundary sharper due to partitioning of elements between minerals.

There are several factors that make the phase boundary broader. First, we can expect a broader transformation in colder, garnet-poor or FeO-rich regions in the mantle based on the equilibrium phase relations. Second, the reaction kinetics at low temperature also tends to broaden the width of the discontinuity since olivine and wadsleyite can coexist metastably under the conditions of a cold subducting slab (e.g., Rubie and Ross 1994; Kubo et al. 1998). Third, the sharpness of the discontinuity may be affected by the presence of water. Wood (1995) used a thermodynamic calculation to estimate that the presence of a small amount of water, i.e., about 100 ppm, can broaden the stability field of coexistence of olivine and wadsleyite by about 3 km. He argued that the sharpness of the 410 km discontinuity indicates that the transition zone is essentially dry. On the other hand, Smyth and Frost (2002) suggested that the hydrogen diffusion and gravitational stratification narrow the phase transformation interval between olivine and wadsleyite, which is an opposite effect from the argument by Wood (1995). The preliminary experiments on determination of the olivine-wadsleyite transformation in peridotite-3.0 wt% water system made by Litasov et al. (2006) suggested that coexistence loop of olivine and wadsleyite expands under the wet conditions, which is consistent with the estimation by Wood (1995). Nolet and Zielhuis (1994), Revenaguh and Sipkin, (1994), and Song et al. (2004) suggested water as a possible cause of anomalies in the deep upper mantle and the transition zone. Recent observations that the width of the 410 km seismic discontinuity beneath the Mediterranean is between 20 and 35 km (Van der Meijde et al. 2003) may be explained by H_2O contents in this region. The cold and wet nature of this area may be supported by the high electrical conductivity of the upper mantle in this region, which is consistent with 1000-1500 ppm H_2O in olivine (Tarits et al. 2004).

The 660 km seismic discontinuity and the post-spinel transformation: average depth and topography of the 660 km seismic discontinuity

The 660 km seismic discontinuity has been considered to be caused by the post-spinel transformation in peridotite (e.g., Ito and Takahashi 1989). Seismological studies show that the 660 km discontinuity is observed globally and the average depth of the discontinuity

is 654 km (Gu and Dziewonski 2002). If we adopt this depth as a global average for the discontinuity, the discrepancy between the pressure of the post-spinel transformation (i.e., decomposition of ringwoodite) determined by experiments and that in seismic studies becomes small. The phase boundary determined experimentally is lower by 0.2-0.3 GPa (i.e., 6-10 km shallower) compared with the pressure of the 660 km discontinuity assuming the temperature of the discontinuity around 1800-2000 K, when we apply the pressure scales of Au and MgO (Tsuchiya 2003; Speziale et al. 2001), which is believed to be the most reliable at present (Figs. 2A,B and Fig. 8). The above small discrepancy may be accounted for by the effect of pressure on the thermocouple EMF, i.e., the temperatures of the high pressure in situ X-ray diffraction study may be underestimated, resulting in a shift of the phase boundary to higher pressure (e.g., Ohtani 1979). The alternative explanation for the discrepancy may be the effect of water on the phase boundary. We observed a change of the Clapeyron slope of the post-spinel phase boundary under hydrous conditions, but found no significant shift of the boundary at higher temperatures around 1773-1873 K as shown in the previous section. On the other hand the boundary appears to shift to higher pressure at lower temperatures; i.e., Higo et al. (2001) and Inoue et al. (2001) reported 0.2 GPa shift of the phase boundary at 1873 K, and Katsura et al. (2003) also suggested 0.6 GPa shift of the post-spinel transition boundary to the higher pressure in hydrous Mg_2SiO_4 based on their preliminary results at 1663 K. Our data indicate that the post-spinel transformation boundary in hydrous pyrolite shifts to higher pressure by about 0.6 GPa relative to anhydrous pyrolite at 1473 K, whereas there is no obvious shift of this boundary at higher temperatures (1773-1873 K).

The Clapeyron slope of the post-spinel transformation determined recently by in situ X-ray diffraction experiments is very gentle (about −0.5 MPa/K) under dry conditions (e.g., Katsura et al. 2003; Fei et al. 2004a; Litasov et al. 2005b). The gentle slope of the post-spinel transformation boundary may require a large temperature difference to account for the topography of the 660 km seismic discontinuity (Figs. 2A,B, Fig. 8).

The depth of the 660 km seismic discontinuity varies by about ±20 km; about +20 km beneath Northern Pacific Ocean, Atlantic Ocean, and South Africa, whereas it is −20 km beneath subduction zones such as the western Pacific and South America (Flanagan and Shearer 1998; Gu and Dziewonski 2002). Lebedev et al. (2003) proposed smaller variations in the range of ±15 km. The depressions caused by the slabs have been studied by many authors; depression of 20~30 km beneath Tonga (Niu and Kawakatsu 1995) and up to about 50 km beneath Izu-Bonin (e.g., Collier et al. 2001). Elevation of the 660 km discontinuity by 10-20 km is also reported in areas related to hot plumes such as Hawaii (Li et al. 2000) and the South Pacific (Niu et al. 2000). If the topography of the discontinuity is caused only by the effect of temperature on the phase boundary, an elevation of 20 km corresponds to a temperature elevation of about 1300 K and a depression of 50 km corresponds to a temperature decrease of about 3000 K, which implies unusually if not impossibly large temperature variations. This indicates that the variation in depth of the 660 km discontinuity cannot be explained only by the temperature effect, but we need to introduce the other effects to explain the topography.

A delay of the phase transformation due to kinetics, or the influence of minor components or volatiles may be additional explanations for the large variations in 660 topography. Kinetics of the post spinel transformation in Mg_2SiO_4 (Kubo et al. 2002a) indicates that the transformation is very fast compared to the speed of the slab subduction and it completes in 10^4 years with 1 GPa of overpressure (i.e., a pressure interval from the equilibrium phase boundary) even at the temperatures of 1000 K (Fig. 7). Only for very cold slabs with temperatures below 1000 K, the post-spinel transformation reaction delays by 10^6-10^8 years, a meaningful duration to explain a large depression of the 660 km discontinuity. We can expect a delay of transformation and shift of the phase boundary by about 1 GPa (corresponding to 20-25 km) due to kinetics only in unusually cold slabs.

The most plausible explanation for such a large elevation and depression of the discontinuity may be the presence of water, although the elevation may be smaller due to lower water solubility in ringwoodite in hot environments. The observed shift of the post-spinel transformation boundary is relevant to the topography of the 660 discontinuity detected by the seismological studies (Fig. 8). The displacement of the post-spinel phase boundary by 0.5 GPa under the hydrous conditions corresponds to about 15 km in depth, which is a half of the observed depressions of the 660 km discontinuity, 30-40 km, in the hot subduction zones at a temperature about 1473 K. Thus, a large displacement of the 660 km discontinuity may be considered as evidence for existence of water in the transition zone (Litasov et al. 2005a,b).

The density relation of basalt and peridotite near the 660 km discontinuity

Ringwood (1994) drew attention to the importance of the density contrast between the basaltic and peridotite layers of a subducting slab. He argued that there is a density crossover between peridotite and basalt due to the pressure difference between the post-spinel transition in the peridotite layer and the post-garnet transition in the basaltic layer of the slabs. Figure 8 summarizes the phase relations of peridotite and basalt under dry and wet conditions and shows the range of temperatures expected for subducting slabs and an average mantle geotherm. Figure 9 shows the density of the peridotite layer and the basalt layer of the slab. Irifune and Ringwood (1993) suggested that the density crossover occurs in the pressure interval of about 2 GPa along the slab geotherm. The density crossover may lead to a separation of the basaltic crust from the peridotite body at a depth of about 660 km resulting in the formation of a garnetite-bearing layer at the base of the transition zone (Ringwood 1994). On the other hand, Hirose et al. (1999) showed that the transformation of the basaltic crust from garnetite to a perovskite lithology occurs near 720 km and they argued that the density crossover between

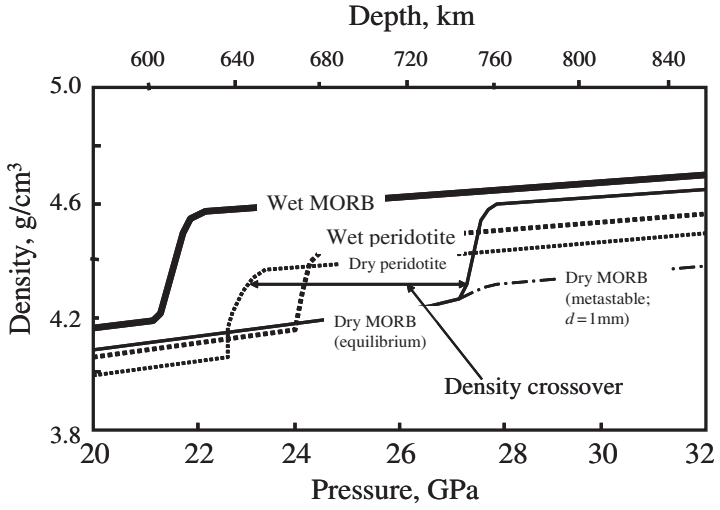

Figure 9. Density profiles of dry and wet basalt (MORB) and pyrolite demonstrating the density crossover near 660 km. Density calculations were carried out along a normal mantle geotherm for anhydrous systems (Akaogi et al. 1989) and a cold subduction geotherm for hydrous systems (Kirby et al. 1996) using a third order Birch-Murnaghan equation of state and the set of thermoelastic parameters given by Litasov and Ohtani (2005). A density crossover exists between the peridotite (thin dotted curve) and basalt (thin solid curve) in the range from 23 GPa to 27 GPa under dry conditions. The sluggish transformation rate of the post-garnet transformation expands the region of the density crossover under dry conditions. There is no density crossover between the peridotite (thick dotted curve) and basalt (thick solid curve) under wet conditions.

basalt and peridotite layers may be too narrow for separation of the basaltic crust to accumulate at the base of the transition zone. Therefore, the basaltic crust may gravitationally sink into the lower mantle. However, the equilibrium phase relations may not be applicable to the phase transformation in real subducting slabs, because reaction kinetics may be an important factor in controlling the mineralogy and density of subducting slabs. Kubo et al. (2002b) studied the kinetics of the post-garnet transformation in basalt, and they showed a very slow reaction rate allowing metastable garnet to survive for a long time (the order of 10 Ma) after crossing the 660 km seismic discontinuity. Therefore, a wider pressure interval of the density crossover can be expected by taking into account the kinetics of the post-garnet transformation under dry conditions, suggesting a separation of the basaltic layer of the slabs to form a garnetite layer at the base of the transition zone (Fig. 9).

Litasov et al. (2004) and Sano et al. (2006) demonstrated that at the low temperature of slabs the density crossover between the peridotite and basalt layers might be absent (Figs. 8 and 9) especially in water-rich subduction zones. The crossover of the post-spinel and post-garnet transformation boundaries locates below the temperature path of a cold subducting slab in anhydrous subduction (point A in Fig. 8), whereas it lies above the temperature path of a hot slab at around 24 GPa and 1500 K (point B in Fig. 8) in hydrous subduction. Therefore, there may be no density crossover between the basalt and peridotite layers of hydrated slabs following cold subduction geotherms. If slabs pass through the 660 km seismic discontinuity, penetration of the basaltic crust component into the lower mantle can occur without gravitational separation from the peridotite body of the slab, at least for hydrous subduction environments.

Seismic reflectors: the possible existence of fluid in the lower mantle

Kaneshima and Helfrich (1998) and Niu et al. (2003) reported seismic reflectors in the lower mantle. Niu et al. (2003) indicate that the physical properties of the reflector observed in the upper part of the lower mantle beneath the Mariana subduction zone show a decrease in shear wave velocity by 2-6% and an increase in density by 2-9% within the reflectors, whereas, no difference exists in P-wave velocity (<1%) between the reflector and the surrounding mantle. The thickness of the reflector is estimated to be around 12 km. The origin of the seismic reflectors is one of the most interesting issues in understanding heterogeneity in the lower mantle. The seismic reflectors may correspond to subducted oceanic crust as was suggested by some authors (e.g., Kaneshima and Helffrich 1999).

In order to test whether subducted oceanic crust can cause these reflections, we need to test whether oceanic crust in the lower mantle can explain the observed seismological properties of the reflectors. There are three possible scenarios that may influence the seismic properties of subducted crust in the lower mantle. First, the subducted crust may possess an equilibrium lower mantle lithology composed of Mg-perovskite, Ca-perovskite, stishovite, and calcium ferrite type aluminous phase (CF) (or Na-aluminous phase, NAL). Second, it may possess a metastable majorite garnet lithology due to the sluggish transformation kinetics of the garnet-perovskite transformation (Kubo et al. 2002b). The third possibility is that the physical properties of the reflectors cannot be accounted for by the above two lithologies, and an additional factor is needed to explain the properties of the reflectors. The factor may be the presence of fluid or magma at these depths.

In order to find a plausible explanation for the properties of the reflectors, we need to estimate physical properties of the oceanic crust under lower mantle conditions. Ohtani (2006) estimated the physical properties of high-pressure minerals in the oceanic crust and mantle. Figure 10 shows the differences between density, v_P, and v_S of the basaltic crust in the slab and the surrounding mantle peridotite. The density and velocity (v_P and v_S) differences between the reflector and surrounding mantle observed seismologically (Niu et al. 2003) are also shown in this figure. The properties of MORB with a metastable garnet-bearing lithology are also shown in this figure. A decrease in v_S and an increase in density are the characteristic

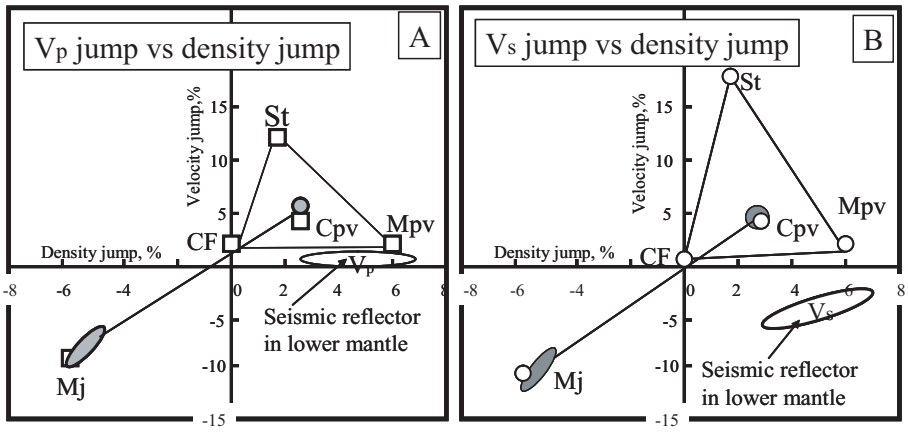

Figure 10. Differences (%) in density and v_P between basalt (MORB) in the slab and surrounding mantle peridotite (A) and those in density and v_S between basalt and peridotite (B). The density and velocity (v_P and v_S) differences between the reflector and surrounding mantle observed seismologically (Niu et al. 2003) are also shown in these figures. Density, v_P, and v_S of the mantle minerals are calculated at conditions of 30 GPa and 1873 K by using the procedure and parameters given in Ohtani (2006). Open squares and circles represent the v_P-density jump and v_S-density jump, respectively. The shaded areas indicate that the density and velocity differences of the majorite bearing assemblage and perovskite bearing assemblage. The properties of the reflectors cannot be explained either by a stable perovskite bearing assemblage nor a metastable majorite bearing assemblage. Abbreviations in the Figure are the same as those given in Figures 3 and 8.

properties of the reflector which cannot be accounted for by either the perovskite lithology or metastable majorite lithology of basalt, i.e., by a complete or incomplete phase transformation from majorite to perovskite lithologies, although there is a large uncertainty in seismic velocity, especially v_S in basalt. The detailed calculations and the error estimations of the v_P and v_S are given in Ohtani (2006). We need additional factors to reduce v_S, although the density increase can be explained by the lower mantle lithology; i.e., the complete phase transformation from majorite lithology to perovskite lithology shows positive jumps in density, v_P and v_S relative to the surrounding mantle, whereas the metastable majorite lithology shows physical properties (ρ, v_P, and v_S) that are smaller than the surrounding mantle. It may be possible to explain the drastic decrease in v_S as an effect of fluid or melt films in the subducted oceanic lithosphere in the lower mantle (e.g., Williams and Garnero 1996).

Hydrous phase D dehydrates at pressures around 40-50 GPa (Shieh et al. 1998). Therefore, the physical properties of the reflectors might be explained by fluid in the oceanic crust supplied from dehydration of this phase in the underlying hydrous peridotite layer of the slab penetrating into the lower mantle. Although the existence of fluid films in the oceanic crust of the slabs is a plausible mechanism for the change of the physical properties of reflectors, the existence of minor metallic iron formed by the garnet-perovskite transformation in the oceanic crust (Miyajima et al. 1999; Frost et al. 2004) could also cause the reduction of shear wave velocity and increase the density of the reflectors. In addition, several other explanations might also account for the unusual properties of the reflectors. Theoretical calculations, for example, have revealed the existence of an elastic anomaly associated with the phase transformation from stishovite to the post-stishovite $CaCl_2$ phase (e.g., Stixrude 1998). A similar anomaly could result from the transformation in Al_2O_3 bearing $CaSiO_3$ perovskite from the orthorhombic to cubic phase (Kurashina et al. 2004). The elastic anomalies associated with theses phase transformations, however, are not yet confirmed experimentally.

CONCLUDING REMARKS

In this chapter we have summarized recent advances in the study of the effects of water on major phase transformations in the Earth's mantle with implications for the topography of seismic discontinuities and mantle dynamics based on the results of quenched multianvil and *in situ* X-ray diffraction experiments at high pressure and temperature. Differences in water solubility between (a) wadsleyite and olivine and (b) ringwoodite and Mg-perovskite and ferropericlase may cause displacement of the phase transition boundaries, which are believed to be responsible for the 410 and 660 km discontinuities, respectively. Experimental results show that water may increase the pressure interval of the binary olivine-wadsleyite transformation loop, i.e., water expands the stability field of wadsleyite to lower pressures. This interval is ~0.3 GPa (or ~6 km) wide at 1700 K in the anhydrous pyrolite, whereas it may be ~1.2 GPa at 1500 K (or 33 km) in pyrolite with 2-3 wt% of H_2O. The broadening of the 410 km discontinuity observed in some regions of the mantle is consistent with enrichment by water in the mantle. A significant shift of the boundary of the wadsleyite to ringwoodite phase transformation to the higher pressure through the addition of water to the peridotite system may also be responsible for variations in the depth of the 520 km discontinuity. However, the cause of a significant displacement of the wadsleyite/ringwoodite phase boundary is not clear.

In situ X-ray diffraction study of the post-spinel transformation in hydrous pyrolite indicates that the phase boundary is shifted to higher pressures by 0.6 GPa relative to anhydrous pyrolite at 1473 K, whereas it shows no obvious shift at higher temperature of around 1873 K. The displacement of the post-spinel phase transformation boundary in hydrous pyrolite would correspond to a depth variation of about 15 km and may account for approximately half of 30-40 km depression observed for the 660 km discontinuity in subduction zones at temperatures of around 1473 K. This effect should be much stronger at lower temperatures. Since the Clapeyron slope of the post-spinel transformation boundary in anhydrous pyrolite is very gentle (about −0.5 MPa/K), we cannot explain depressions of the 660 km discontinuity as a result of temperature variations alone. Thus, a large depression of the 660 km discontinuity might be considered as direct evidence for the existence of water in the transition zone.

In situ X-ray diffraction studies of the post-garnet transformation in anhydrous and hydrous basalt show that the phase boundary shifts to lower pressures by ~2 GPa upon the addition of water. This observation demonstrates that at temperatures of subducting slabs the density crossover between peridotite and basalt near 660 km might be absent under hydrous conditions. The basaltic component of the slab may therefore penetrate into the lower mantle under hydrous conditions and not separate from the peridotite body at the 660 km discontinuity.

ACKNOWLEDGMENTS

We thank A. Suzuki, T. Kubo, H. Terasaki, K. Funakoshi, T. Kondo for collaboration during the experiments at SPring-8. We appreciate S.D. Jacobsen and an anonymous reviewer for improving the manuscript. This work was supported by the grants in Aid for Scientific Researches from the Ministry of Education, Culture, Sports, Science and Technology, Japan (No. 14102009 and 16075202) to E. Ohtani. This work was conducted as a part of the 21th Century Center-of-Excellence program Advanced Science and Technology Center for the Dynamic Earth at Tohoku University.

REFERENCES

Agee CB (1998) Phase transformations and seismic structure in the upper mantle and transition zone. Rev Mineral 37:165-203

Akaogi M, Ito E, Navrotsky A (1989) Olivine-modified spinel-spinel transitions in the system Mg_2SiO_4-Fe_2SiO_4: calorimetric measurements, thermochemical calculation, and geophysical application. J Geophys Res 94:15671-15685

Anderson OL, Issak DG, Yamamoto S (1989) Anharmonicity and the equation state for gold. J Appl Phys 6: 1534-1543

Bell DR, Rossman GR, Maldener J, Endisch D, Rauch F (2003) Hydroxide in olivine: A quantitative determination of the absolute amount and calibration of the IR spectrum. J Geophys Res 108, doi: 10.1029/2001JB000679

Benz HM, Vidale JE (1993) Sharpness of upper-mantle discontinuities determined from high-frequency reflections. Nature 365:147-150

Bina CR, Helffrich GR (1994) Phase transition Clapeyron slopes and transition zone seismic discontinuity topography. J Geophys Res 99:15853-15860

Bolfan-Casanova N, Keppler H, Rubie DC (2000) Water partitioning between nominally anhydrous minerals in the MgO-SiO_2-H_2O system up to 24 GPa: implications for the distribution of water in the Earth's mantle. Earth Planet Sci Lett 182:209-221

Bolfan-Casanova N, Mackwell S, Keppler H, McCammon C, Rubie DC (2002) Pressure dependence of H solubility in magnesiowüstite up to 25 GPa: Implications for the storage of water in the Earth's lower mantle. Geophys Res Lett 29, doi: 10.1029/2001GL014457

Bolfan-Casanova N, Keppler H, Rubie DC (2003) Water partitioning at 660 km depth and evidence for very low water solubility in magnesium silicate perovskite. Geophys Res Lett 30, doi: 10.1029/2003GL017182

Brown JM (1999) High pressure equation of state for NaCl, KCL, and CsCl. J Appl Phys 86:5801-5808

Chen J, Inoue T, Weidner DJ, Wu Y (1998) Strength and water weakening of mantle minerals, α, β, and γ Mg_2SiO_4. Geophys Res Lett 25:575-578

Chen J, Inoue T, Yurimoto H, Weidner DJ (2002) Effect of water on olivine-wadsleyite phase boundary in the (Mg,Fe) SiO system. Geophys Res Lett 29:1875, doi:10.1029/2001 GL014429

Chudinovskikh L, Boehler R (2001) High-pressure polymorphs of olivine and the 660 km seismic discontinuity. Nature 411:574-577

Chung JI, Kagi H (2002) High concentration of water in stishovite in the MORB system. Geophys Res Lett 29, doi: 10.1029/2002GL015579

Collier JD, Helffrich GR, Wood BJ (2001) Seismic discontinuities and subduction zones. Phys Earth Plane Inter 127:35-49

Demouchy S, Deloule E, Frost DJ, Keppler H (2005) Pressure and temperature dependence of water solubility in Fe-free wadsleyite. Am Mineral 90:1084-1091

Dziewonski AM, Anderson DL (1981) Preliminary Reference Earth Model. Phys Earth Planet Int 25:297-356

Fei Y, Van Orman J, Li J, van Westrenen W, Sanloup C, Minarik W, Hirose K, Komabayashi K, Walter M, Funakoshi K (2004a) Experimentally determined postspinel transformation boundary in Mg_2SiO_4 using MgO as an internal pressure standard and its geophysical implications. J Geophys Res 109, doi: 10.1029/2003JB002562

Fei Y, Li J, Hirose K, Minarik W, Van Orman J, Sanloup C, van Westrenen W, Komabayashi T, Funakoshi K (2004b) A critical evaluation of pressure scales at high temperatures by *in situ* X-ray diffraction measurements. Phys Earth Planet Inter 143-144:515-526

Flanagan MP, Shearer PM (1998) Global mapping of topography on transition zone velocity discontinuities by stacking SS precursors. J Geophys Res 103:2673-2692

Flanagan MP, Shearer PM (1999) A map of topography on the 410 km discontinuity from PP precursors. Geophys Res Lett 26:549-552

Frost DJ (2003) The structure and sharpness of $(Mg,Fe)_2SiO_4$ phase transformations in the transition zone. Earth Planet Sci Lett 216:313-328

Frost DJ, Liebske C, Langenhorst F, McCammon C, Tronnes RG, Rubie DC (2004) Experimental evidence of iron-rich metal in the Earth's lower mantle. Nature 428:409-411

Fukao Y, Koyama T, Obayashi M, Utada H (2004) Trans-Pacific temperature field in the mantle transition zone derived from seismic and electromagnetic tomography. Earth Planet Sci Lett 217:425-434

Gu YJ, Dziewonski AM (2002) Global variability of transition zone thickness. J Geophys Res 107, doi: 10/1029/2001JB000489

Gu YJ, Dziewonski AM, Agee CB (1998) Global de-correlation of the topography of the transition zone discontinuity. Earth Planet Sci Lett 157:57-67

Hae R, Ohtani E, Kubo T, Koyama T, Utada H (2006) Hydrogen diffusivity in wadsleyite and water distribution in the mantle transition zone. Earth Planet Sci Lett 243:141–148

Higo Y, Inoue T, Irifune T, Yurimoto H (2001) Effect of water on the spinel post-spinel transformation in Mg_2SiO_4. Geophys Res Lett 28:3505-3508

Hirose K (2002) Phase transitions in pyrolitic mantle around 670 km depth: implications for upwelling of plumes from the lower mantle. J Geophys Res 107, doi: 10.1029/2001JB000597

Hirose K, Fei Y (2002) Subsolidus and melting phase relations of basaltic composition in the uppermost lower mantle. Geochim Cosmochim Acta 66:2099-2108

Hirose K, Fei Y, Ma Y, Mao HK (1999) The fate of subducted basaltic crust in the Earth's lower mantle. Nature 397:53-56

Hirth G, Kohlstedt DL (1996) Water in the oceanic upper mantle: Implications for rheology, melt extraction and the evolution of the lithosphere. Earth Planet Sci Lett 144:93-108

Hosoya T, Kubo T, Ohtani, E, Sano A, Funakoshi K (2005) Water controls the fields of metastable olivine in cold subducting slabs. Geophys Res Lett 32:L17305 doi:10.1029/2005GL023398

Inoue T (1994) Effect of water on melting phase relations and melt compositions in the system Mg_2SiO_4-$MgSiO_3$-H_2O up to 15 GPa. Phys Earth Planet Inter 85:237-263

Inoue T, Weidner DJ, Northrup PA, Parise JB (1998) Elastic properties of hydrous ringwoodite (γ-phase) in Mg_2SiO_4. Earth Planet Sci Lett 160:107–113

Inoue T, Higo Y, Ueda T, Tanimoto Y, Irifune T (2001) The effect of water on the high-pressure phase boundaries in the system Mg_2SiO_4-Fe_2SiO_4. Transport of Materials in the Dynamic Earth, Kurayoshi, p 128-129

Inoue T, Tanimoto Y, Irifune T, Suzuki T, Fukui H, Ohtaka O (2004) Thermal expansion of wadsleyite, ringwoodite, hydrous wadsleyite and hydrous ringwoodite. Phys Earth Planet Inter 143-144:279-290

Irifune T, Ringwood AE (1993) Phase transformations in sbducted oceanic crust and buoyancy relationships at depths of 600-800 km in the mantle. Earth Planet Sci Lett 117:101-110

Irifune T, Nishiyama N, Kuroda K, Inoue T, Isshiki M, Utsumi W, Funakoshi K, Urakawa S, Uchida T, Katsura T, Ohtaka O (1998) The postspinel phase boundary in Mg_2SiO_4 determined by *in situ* X-ray diffraction. Science 279:1698-1700

Ito E, Takahashi E (1989) Post-spinel transformation in the system Mg_2SiO_4-Fe_2SiO_4 and some geophysical implications. J Geophys Res 94:10637-10646

Jacobsen SD, Smyth JR, Spetzler H, Holl CM, Frost DJ (2004) Sound velocities and elastic constants of iron-bearing hydrous ringwoodite. Phys Earth Planet Inter 143-144:47-56

Jamieson JC, Fritz JN, Manghnani MH (1982) Pressure measurements at high temperature in X-ray diffraction studies: gold as a primary standard. *In*: High pressure research in geophysics. Akimoto S, Manghnani MH (ed) Center for Academic Publications Japan, Tokyo, p 27-48

Kaneshima S, Helffrich G (1998) Detection of lower mantle scatterers northeast of the Mariana subduction zone using short-period array data. J Geophys Res 103:4825-4838

Kaneshima S, Helffrich G (1999) Dipping lower-velocity layer in the mid-lower mantle: evidence for geochemical heterogeneity. Science 283:1888-1891

Karato S (1989) Grain growth kinetics in olivine aggregates. Tectonophysics 168:255- 273

Karato S (1990) The role of hydrogen in the electrical conductivity of the upper mantle. Nature 347: 72–273

Katayama I, Hirose K, Yurimoto H, Nakashima S (2003) Water solubility in majoritic garnet in subduction oceanic crust. Geophys Res Lett 30, doi: 10.1029/2003GL018127

Katsura T, Ito E (1989) The system Mg_2SiO_4-Fe_2SiO_4 at high pressures and temperatures: Precise determination of stabilities of olivine, modified spinel, and spinel. J Geophys Res 94:15663-15670

Katsura T, Yamada H, Shinmei T, Kubo A, Ono S, Kanzaki M, Yoneda A, Walter MJ, Ito E, Urakawa S, Funakosh Ki, Utsumi W (2003) Post-spinel transition in Mg_2SiO_4 determined by high P-T *in situ* X-ray diffraction. Phys Earth Planet Inter 136:11-24

Katsura T, Yamada H, Nishikawa O, Song M, Kubo A, Shinmei T, Yokoshi S, Aizawa Y, Yoshino T, Walter MJ, Ito E, Funakoshi K (2004) Olivine-wadsleyite transition in the system $(Mg,Fe)_2SiO_4$. J Geophys Res 109: B02209, doi:10.1029/2003JB002438

Kawamoto T (2004) Hydrous phase stability and partial melt chemistry in H_2O-saturated KLB-1 peridotite up to the uppermost lower mantle conditions. Phys Earth Planet Inter 143-144:387-395

Kawamoto T, Matsukage K, Mibe K, Isshik M, Nishimura K, Ishimatsu N, Ono S (2004) Mg/Si ratios of aqueous fluids coexisting with forsterite and enstatite based on the phase relations in the Mg_2SiO_4-SiO_2-H_2O system. Am Mineral 89:1433-1437

Kerschhofer L, Rubie DC, Sharp TG, McConnell JDC, Dupas-Bruzek C (2000) Kinetics of intercrystalline olivine-ringwood transformation. Phys Earth Planet Inter 121:59-76

Kirby SH, Stein S, Okal EA, Rubie DC (1996) Metastable mantle phase transformations and deep earthquakes in subducting oceanic lithosphere. Rev Geophys 34:261-306

Koyama T, Shimizu H, Utada H, Ohtani E, Hae R (2006) Water contents in the mantle transition zone beneath the north Pacific derived from the electrical conductivity anomaly. *In*: Earth's Deep Water Cycle. Jacobsen S, van der Lee S (eds) Am Geophys Union Monogr (in press)

Kohlstedt DL, Keppler H, Rubie DC (1996) Solubility of water in the α, β, and γ phases of $(Mg,Fe)_2SiO_4$. Contrib Mineral Petrol 123:345-357

Koper KD, Wiens DA, Dorman LM, Hildebrand JA, Webb SC (1998) Modeling the Tonga slab: can travel time data resolve a metastable olivine wedge? J Geophys Res 103:30079-30100

Kubo A, Akaogi M (2000) Post-garnet transitions in the system $Mg_4Si_4O_{12}$-$Mg_3Al_2Si_3O_{12}$ up to 28 GPa: phase relations of garnet, ilmenite and perovskite. Phys Earth Planet Inter 121:85-102

Kubo T, Ohtani E, Kato T, Shinme T, Fujino K (1998) Effect of water on the α-β transformation kinetics in San Carlos Olivine. Science 281:85–87

Kubo T, Ohtani E, Kato T, Urakawa S, Suzuki A, Kanbe Y, Funakoshi K, Utsumi W, Kikegawa T, Fujino K (2002a) Mechanism and kinetics of the post-spinel transformation in Mg_2SiO_4. Phys Earth Planet Inter 129:153-171

Kubo T, Ohtani E, Kondo T, Kato T, Toma M, Hosoya T, Sano A, Kikegawa T, Nagase T (2002b) Metastable garnet in oceanic crust at the top of the lower mantle. Nature 420:803-806

Kubo T, Ohtani, E Funakoshi K (2004) Nucleation and growth kinetics of the α-β transformation in Mg_2SiO_4 determined by *in situ* synchrotron powder X-ray diffraction. Am Mineral 89:285-293

Kurashina T, Hirose K, Ono S, Sata N, Ohishi Y (2004) Phase transition in Al-bearing $CaSiO_3$ perovskite: implications for seismic discontinuities in the lower mantle. Phys Earth and Planet Inter 145:67-74

Kurosawa M, Yurimoto H, Sueno S (1997) Patterns in the hydrogen and trace element compositions of mantle olivines. Phys Chem Mineral 24:385-395

Lebedev S, Chevrot S, van der Hilst RD (2003) Correlation between the shear-speed structure and thickness of the mantle transition zone. Phys Earth Planet Inter 136:25-40

Li X, Kind R, Priestley K, Sobolev SV, Tilmann F, Yuan X, Weber M (2000) Mapping the Hawaiian plume conduit with converted seismic waves. Nature 405:938-941

Litasov KD, Ohtani E (2003) Stability of hydrous phases in CMAS-pyrolite-H_2O system up to 25 GPa. Phys Chem Mineral 30:147-156

Litasov KD, Ohtani E, Langenhorst F, Yurimoto H, Kubo T, Kondo T (2003) Water solubility in Mg-perovskites and water storage capacity in the lower mantle. Earth Planet Sci Lett 211:189-203

Litasov KD, Ohtani E, Suzuki A, Kawazoe T, Funakoshi K (2004) Absence of density crossover between basalt and peridotite in the cold slabs passing through 660 km discontinuity. Geophys Res Lett 31, doi:10.1029/2004GL021306

Litasov KD, Ohtani E (2005) Phase relations in hydrous MORB at 18-28 GPa: implications for heterogeneity of the lower mantle. Phys Earth Planet Inter 150:239-263

Litasov KD, Ohtani E, Sano A, Suzuki A, Funakoshi K (2005a) Wet subduction versus cold subduction. Geophys Res Lett 32:L13312, doi:10.1029/2005GL022921

Litasov KD, Ohtani E, Sano A, Suzuki A, Funakoshi K (2005b) *In situ* X-ray diffraction study of post-spinel transformation in a peridotite mantle: Implication to the 660 km discontinuity. Earth Planet Sci Lett 238: 311-328

Litasov KD, Ohtani E, Sano A (2006) Influence of water on major phase transitions in the earth's mantle. *In*: Earth's Deep Water Cycle. Jacobsen S, van der Lee S (eds) Am Geophys Union Monogr (in press)

Liu M, Kerschhofer L, Mosenfelder JL, Rubie DC (1998) The effect of strain energy on growth rates during the olivine–spinel transformation. J Geophys Res 103:23897-23909

Matsui M, Parker SC, Leslie M (2000) The MD simulation of the equation of state of MgO: application as a pressure calibration standard at high temperature and high pressure. Am Mineral 85:312-316

Matsukage KN, Jing Z, Karato S (2005) Density of hydrous silicate melt at the conditions of Earth's deep upper mantle. Nature 438:488-491, doi: 10.1038/nature04241

McCammon C (1997) Perovskite as a possible sink for ferric iron in the lower mantle. Nature 387:694-696

Mei S, Kohlstedt DL (2000) Influence of water on plastic deformation of olivine aggregates. 1. Diffusion creep regime. J Geophys Res 105:21457-21470

Miyajima N, Fujino K, Funamori N, Kodo T, Yagi T (1999) Garnet-perovskite transformation under conditions of the Earth's lower mantle: an analytical transmission electron microscopy study. Phys Earth Planet Inter 116:117-131

Morishima H, Kato T, Suto M, Ohtani E, Urakawa S, Utsumi W, Shimomura O, Kikegawa T (1994) The phase boundary between α- and β-Mg_2SiO_4 determined by *in situ* X-ray observation. Science 265:1202-1203

Mosenfelder JL, Marton FC, Ross CR II, Kershhofer R, Rubie DC (2001) Phys Earth Planet Inter 127:165-180

Nishiyama N, Irifune T, Inoue T, Ando J, Funakoshi K (2004) Precise determination of phase relations in pyrolite across the 660 km seismic discontinuity by *in situ* X-ray diffraction and quench experiments. Phys Earth Planet Inter 143-144:185-199

Niu F, Kawakatsu H (1995) Direct evidence for the undulation of the 660 km discontinuity beneath Tonga: Comparison of Japan and California array data. Geophys Res Lett 22:531-534

Niu F, Kawakatsu H, Fukao Y (2003) A slightly dipping and strong seismic reflector at mid-mantle depth beneath the Mariana subduction zone. J Geophys Res 108, doi:10.1029/2002JB002384

Niu F, Inoue H, Suegetsu D, Kanjo K (2000) Seismic evidence for a thinner mantle transition zone beneath the South Pacific Superswell. Geophys Res Lett 27:1981-1984

Nolet G, Zielhuis, A (1994) Low S velocities under the Tornquist-Teisseyre zone: Evidence for water injection into the transition zone by subduction. J Geophys Res 99:15813-15821, doi: 10.1029/94JB00083

Oguri K, Funamor N, Uchida T, Miyajima N, Yagi T, Fujino K (2000) Post-garnet transition in a natural pyrope: a multi-anvil study based on *in situ* X-ray diffraction and transmission electron microscopy. Phys Earth Planet Inter 122:175-186

Ohtani E (1979) Melting relation of Fe_2SiO_4 up to about 200 kbar. J Phys Earth 27:189-203
Ohtani E (2006) Recent progress in experimental mineral physics: phase relations of hydrous systems and the role of water in slab dynamics. *In*: Earth's deep mantle: Structure, Composition, and evolution. Geophys Monograph Series 160. van der Hilst RD, Bass J, Matas J, Trampert J (eds), Am Geophys Union, p 321-334
Ohtani E, Touma M, Litasov K, Kubo T, Suzuki A (2001) Stability of hydrous phases and water storage capacity in the transitional zone and lower mantle. Phys Earth Planet Inter 124:105-117
Ohtani E, Litasov K, Hosoya T, Kubo T, Kondo T (2004) Water transport into the deep mantle and formation of a hydrous transition zone. Phys Earth Planet Inter 143-144:255-269
Paterson MS (1982) The determination of hydroxyl by infrared absorption in quartz. silicate glasses and similar materials. Bull Mineral 105:20-29
Revenaugh, J, Sipkin SA (1994) Seismic evidence for silicate melt atop the 410 km mantle discontinuity. Nature 369:474-476
Ringwood AE (1994) Role of the transition zone and 660 km discontinuity in mantle dynamics. Phys Earth Planet Inter 86:5-24
Rubie DC, Thompson AB (1985) Metamorphic Reactions: Kinetics, Textures, and Deformation. *In*: Advances in Physical Geochemistry. Vol 4. Thompson AB, Rubie DC (eds) Springer-Verlag, p 27-79
Rubie DC, Ross II CR (1994) Kinetics of the olivine-spinel transformation in subducting lithosphere: experimental constraints and implications for deep slab processes. Phys Earth Planet Inter 86:223-241
Sano A, Ohtani E, Litasov KD, Kubo T, Hosoya T, Funakoshi K, Kikegawa T (2006) Effect of water on garnet-perovskite transformation in MORB and implications for penetrating slab into the lower mantle. Phys Earth Planet Inter (in press)
Sakamaki T, Suzuki A, Ohtani E (2006) Stability of hydrous melt at the base of the Earth's upper mantle. Nature 439:192-194
Shearer PM (1996) Transition zone velocity gradients and the 520 km discontinuity. J Geophys Res 101:3053-3066
Shearer PM (2000) Upper mantle seismic discontinuities. *In*: Earth's Deep Interior: Mineral Physics and Tomography from the Atomic to the Global Scale. Geophysical Monograph 117. Karato S, Forte AM, Liebermann RC, Masters G, Stixrude L (eds) Am Geophys Union, p 115-131
Shieh SR, Mao HK, Ming JC (1998) Decomposition of phase D in the lower mantle and the fate of dense hydrous silicates in subducting slabs. Earth Planet Sci Lett 159:13-23
Shim SH, Duffy TS, Shen G (2001) The post-spinel transformation in Mg_2SiO_4 and its relation to the 660 km seismic discontinuity. Nature 411:571-574
Shim SH, Duffy TS, Takemura K (2002) Equation of state of gold and its application to the phase boundaries near 660 km depth in Earth's mantle. Earth Planet Sci Lett 203:729-739
Smyth J, Frost DJ (2002) The effect of water on the 410 km discontinuity: An experimental study. Geophys Res Lett 29, doi:10.1029/2001GL014418
Song TR, Helmberger DV, Grand SP (2004) Low-velocity zone atop the 410 km seismic discontinuity in the northwestern United States. Nature 427:530-533
Speziale S, Zha CS, Duffy TS, Hemley RJ, Mao HK (2001) Quasi-hydrostatic compression of magnesium oxide to 52 GPa: implication for the pressure-volume-temperature equation of state. J Geophys Res 106: 515-528
Stixrude L (1998) Elastic constants and anisotropy of $MgSiO_3$ perovskite, periclase, and SiO_2 at high pressure. *In*: Core-Mantle Boundary Region. Geodynamics Series 28. Gurnis M, Wysession ME, Knittle E, Biffet BA (eds) Am Geophys Union, p 83-96
Suzuki A, Ohtani E, Morishima H, Kubo T, Kanbe Y, Kondo T, Okada T, Terasaki H, Kato T, Kikegawa T (2000) *In situ* determination of the phase boundary between wadsleyite and ringwoodite in Mg_2SiO_4. Geophys Res Lett 27:803–806
Tarits P, Hautot S, Perrier F (2004) Water in the mantle: Results from electrical conductivity beneath the French Alps. Geophys Res Lett 31, doi:10.1029/2003GL019277
Tsuchiya T (2003) First-principles prediction of the P-V-T equation of state of gold and the 660 km discontinuity in Earth's mantle. J Geophys Res 108, doi:10.1029/2003JB002446
Turnbull D (1956) Phase changes, in Solid State Physics. Vol 3. Seitz F, Turnbull D (eds) Elsevier, p 225-306
Van der Meijde M, Marone F, Giardini D, van der Lee S (2003) Seismic evidence for water deep in the Earth's upper mantle. Science 300:1556-1558
Weidner DJ, Wang Y (2000) Phase transformations: Implications for mantle structure Earth's Deep Interior. *In*: Earth's Deep Interior: Mineral Physics and Tomography from the Atomic to the Global Scale. Geophysical Monograph Vol. 117. Karato S, Forte AM, Liebermann RC, Masters G, Stixrude L (eds) Am Geophys Union, p 215-235
Williams Q, Garnero EJ (1996) Seismic evidence for partial melting at the base of the lower mantle. Science 273:1528-1530
Wood BJ (1995) The effect of H_2O on the 410-kilometer seismic discontinuity. Science 268*:*74-76